Inter-ELM power losses and their dependence on pedestal parameters in JET C- and ITER-like wall H-mode plasmas

A. R. Field¹, L. Frassinetti², C. Maggi¹, S. Saarelma¹ and JET contributors*

EUROfusion Consortium, JET, Culham Science Centre, Abingdon, OX14 3DB, UK.

¹CCFE, Culham Science Centre, Abingdon, OX14 3DB, UK.

²Association VR, Fusion Plasma Physics, KTH, SE-10044, Stockholm, Sweden.

*see the author list of X. Litaudon et al., Nucl. Fusion 57 (2017) 102100

Results of empirical, power-balance calculations of the inter-ELM loss power across the separatrix P_{sep}^{iELM} are presented for JET pulses with both the carbon- (JET-C) and ITER-like (JET-ILW) walls, for comparison with results of on-going, non-linear, gyro-kinetic calculations of pedestal heat transport, e.g. as reported in [1, 2]. Such studies might explain the generally lower pedestal temperatures prevailing in JET-ILW H-mode pulses compared to those in JET-C pulses at the same I_p/B_t and confinement factor H_{98} , despite requiring double the input power in the JET-ILW pulses to achieve the same pedestal pressure.

It is important to quantify the inter-ELM loss power P_{sep}^{iELM} because this is comparable to the ELM-loss power $\langle P_{ELM} \rangle$ (averaged over many ELM cycles) and it is deposited in localised regions close to the strike points, requiring sweeping of their location to prevent melting of the targets at high input power. The relation between P_{sep}^{iELM} and the pedestal parameters (T_e , n_e and p_e at the top of the edge transport barrier (ETB)) and their gradients is also investigated to provide further input for comparison with the GK calculations.

In high-power, 3.0 MA JET-ILW pulses, the fraction of input power lost by radiation ($\mathcal{F}_{Rad} \sim 30\text{-}40\%$) is about double that in JET-C pulses with similar pedestal pressure ($\mathcal{F}_{Rad} \sim 15\text{-}20\%$), which is achieved with much lower input power ($\sim 60\%$) than in the JET-ILW pulses. Such JET-ILW pulses with absorbed power $P_{Abs} \geq 25$ MW exhibit a highly asymmetric radiation distribution, which peaks at the low-field side (LFS) of the peripheral 'mantle' region ($\rho_N > 0.7$). We show this to be consistent with the poloidal re-distribution of a dominant W impurity within flux surfaces by toroidal rotation. Such a strongly asymmetric, mantle radiation is not observed in the lower power (< 16 MW), low-current (1.4 MA) pulses discussed below.

The residual loss-power crossing the separatrix P_{Sep} is calculated from the power balance: $P_{Sep} = P_{Abs} - P_{Rad}^{Pl} - dW_{pl}/dt$, where P_{Abs} is the absorbed power and W_{pl} is the plasma stored energy. (In a steady state H-mode plasma, dW_{pl}/dt must be equal the time-averaged ELM loss power $\langle P_{ELM} \rangle$ to maintain a constant $\langle W_{pl} \rangle$ averaged over many ELM cycles.) The power radiated from the confined plasma P_{Rad}^{Pl} is determined from tomographic inversions of multi-chord bolometer data. To estimate the stored energy W_{pl} , we use W_{MHD} obtained from fast (0.5 ms) EFIT equilibrium reconstructions.

In JET-ILW, the time response of internal magnetic signals used as input to EFIT is delayed by several ms, making the determination of ELM energy losses from W_{MHD} less reliable than for JET-C pulses. Comparison of ΔW_{MHD} with ELM losses determined from pre- and post-ELM profile fits to high-resolution Thomson scattering (TS) data (ΔW_{kin}), shows ΔW_{MHD} overestimates ΔW_{kin} by a factor ≤ 1.25 for ELM frequencies $f_{ELM} \leq 40$ Hz but underestimates ΔW_{ELM} by a factor ≥ 0.4 at higher ELM frequencies, for which the time delay becomes comparable to the inter-ELM period, τ_{ELM} . By averaging the P_{Sep} data from power balance over many inter-ELM periods, it is thereby possible to determine a reasonable estimate of P_{Sep}^{IELM} for JET-ILW pulses with f_{ELM} below 40 Hz.

First, we concentrate on a series of low plasma current (1.4 MA/1.7T), type-I ELMy H-mode, JET-ILW pulses with a range of input powers [3]. Although the type-I ELM frequency

increases with P_{Abs} , at the lowest gas fuelling rate ($\Gamma_{D2} \sim 3 \times 10^{21}$ e/s), f_{ELM} remains low enough (≤ 40 Hz) for ΔW_{ELM} to be determined from EFIT (at higher fuelling rates, f_{ELM} is generally higher and the analysis more unreliable).

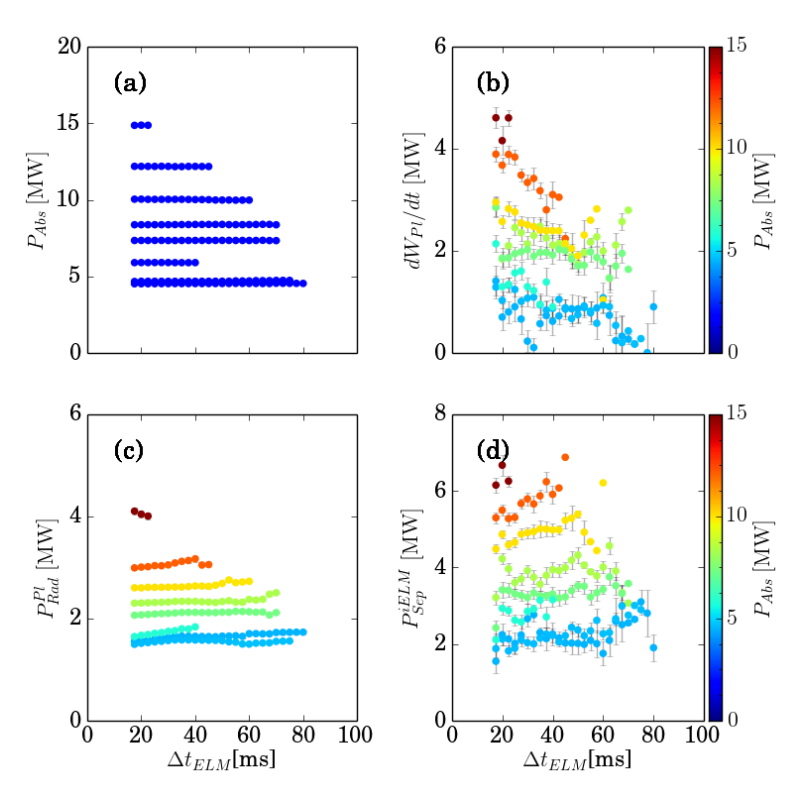


Fig. 1 Inter-ELM power balance for the 1.4 MA/1.7T, low-gas JET-ILW pulses #84971-8 showing: (a) absorbed power, P_{Abs} ; (b) rate of change of plasma energy, dW_{pl}/dt ; (c) radiated power, P_{Rad}^{Pl} ; and (d) separatrix loss power, P_{Sep}^{IELM} as a function of time from the previous ELM, Δt_{ELM} , where the colours represent P_{Abs} .

The components of the inter-ELM power balance for this series of pulses are shown in Fig. 1. Radiation and ELMs each account for ~ 20-30% of the total absorbed power, with the residual, inter-ELM pedestal transport accounting for the remainder. As P_{abs} increases from 4.5 to 16 MW, the powers in all three loss-channels increase in proportion, with P_{sep}^{iELM} rising from ~ 2 to 6 MW. (Note that early in the inter-ELM period for $\Delta t_{ELM} \leq 20$ ms, unreliable P_{sep}^{iELM} data is excluded.)

The dependence of P_{sep}^{iELM} on pedestal parameters is investigated by subtracting the time of the previous ELM from that of the HRTS profile data at each laser pulse. Broadly consistently with results in [4, 5], as P_{Abs} is increased (4.5 \rightarrow 16 MW): at

the pedestal top, $T_{e,ped}$ approximately doubles, while $n_{e,ped}$ decreases by ~ 25%, with similar changes to their gradients. These changes double $\eta_e \equiv L_{n_e}/L_{T_e}$, which saturates at ~ 2 and the pressure at the pedestal top $p_{e,ped}$ reaches at a higher pre-ELM value (2 \rightarrow 4 kPa), which indicates that gradient-driven transport may be limiting $dp_{e,ped}/dr$ rather than MHD stability.

As shown in Fig 2, both $p_{e,ved}$ $dp_{e,ped}/d\psi_N$ increase with P_{sep}^{iELM} as expected for pressure-gradient driven transport across the ETB. This spread of data is un-correlated with the normalised inter-ELM time $\Delta \tau_{ELM} =$ $\Delta t_{ELM}/\tau_{ELM}$ because most of the pedestal recovery occurs during the first 20 ms when the P_{sep}^{iELM} data is unreliable.

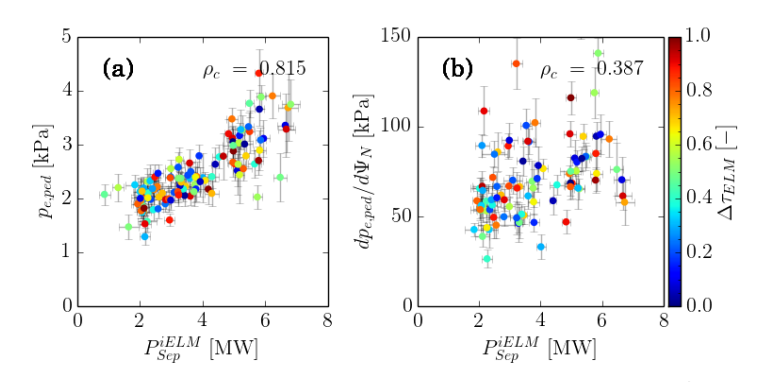


Fig. 2 The dependence of: (a) $p_{e,ped}$ and (b) $dp_{e,ped}/d\psi_N$ on P_{Sep}^{iELM} for the pulses shown in Fig. 1, where the colour represents $\Delta \tau_{ELM}$.

It should be noted that these estimates of P_{sep}^{iELM} from power balance include charge-exchange losses, which are expected to be of order 1 MW, requiring further modelling to quantify.

Next, we compare the loss-powers and pedestal parameters in high-power, 3.0 MA JET-C and JET-ILW pulses with similar confinement factor H_{98} ~ 1. In the JET-ILW pulses considerably

Pulse	Wall	I_p	$\boldsymbol{B_t}$	q_{95}	δ	Γ_{D2}	P_{Abs}	$\boldsymbol{\beta}_N$	H_{98}
#	-	MA	T	-	-	$10^{22}/s$	MW	-	-
78677	C	3.0	2.6	2.6	0.24	-	17.8	1.8	1.0
78697	C	3.0	2.6	2.6	0.24	-	14.7	1.8	1.0
92300	Be/W	3.0	2.7	3.0	0.2	2.5	32.1	1.9	0.9
92432	Be/W	3.0	2.7	3.0	0.2	1.9	32.0	2.2	1.0

Table 1. Parameters of high-performance JET-C and JET-ILW pulses at 3.0 MA plasma current used for power-balance calculations and in Fig 3.

more heating is required ($P_{Abs} \sim 32$ MW) to achieve the same pedestal pressure as in the JET-C (~ 18 MW) pulses. Whereas in JET-C pulses no gas fuelling was needed during the steady-state phase, significant gas fuelling is required for sustained operation in JET-ILW. Although a higher gas fuelling rate Γ_{D2} controls the W influx, it increases f_{ELM} and degrades confinement, reducing the pedestal temperature $T_{e,ped}$, requiring more power to achieve the same pedestal pressure as in the JET-C pulses [4], these effects worsening with increasing puffing rate.

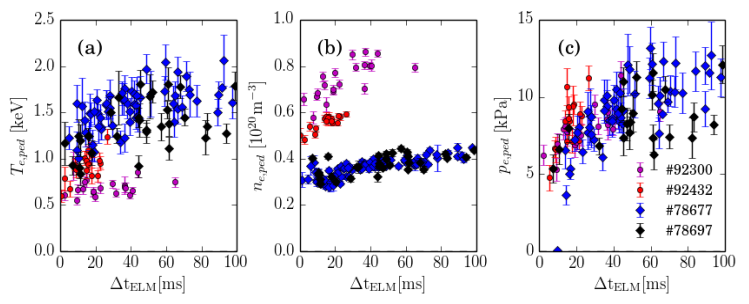


Fig. 3 Parameters at the pedestal top: (a) $T_{e,ped}$; (b) $n_{e,ped}$ and (c) $p_{e,ped}$ from fits to HRTS profile data as a function of time after the previous ELM peak Δt_{ELM} for the JET-ILW and -C pulses shown in Fig. 3.

As shown in Fig. 3, the pre-ELM pedestal $T_{e,ped} \sim 0.7\text{-}1.0$ keV is about half of that in the JET-ILW pulses than in the JET-C pulses, while $n_{e,ped} \sim$ $0.6\text{-}0.8\times10^{20}$ m⁻³ is higher (c.f. 0.4×10^{20} m⁻³ in JET-C), resulting in a comparable pre-ELM $p_{e,ped} \sim 10$ kPa.

Results of inter-ELM power balance calculations for these

pulses are summarised in Table 2, which also states the fraction of power \mathfrak{F}_{x} lost in each channel x relative to P_{Abs} . We do not show a figure like Fig. 1 for these pulses because the detailed time dependence of P_{sep}^{iELM} is not reliable for the JET-ILW pulses, especially for #92432 in which $f_{ELM} \sim 40$ Hz. Instead, in Table 2, we quote average values of each loss component during the inter-ELM period, including uncertainties, which are dominated by noise on the dW_{MHD}/dt term.

Pulse	Wall	P_{Abs}	P_{Rad}	$\langle P_{ELM} \rangle$	P_{Sep}^{iELM}	\mathfrak{F}_{Rad}	\mathfrak{F}_{ELM}	F Sep
#	-	MW	MW	MW	MW	ı	ı	-
78677	C	17.85±0.00	3.94 ± 0.01	7.29 ± 0.14	6.62 ± 0.13	0.21	0.50	0.29
78697	C	14.70±0.00	2.06±0.02	6.91±0.16	5.69±0.16	0.15	0.53	0.33
92300	Be/W	32.06±0.05	12.3±0.02	6.76±0.31	13.0±0.28	0.37	0.21	0.44
92432	Be/W	32.02±0.19	9.50±0.18	10.9±0.43	11.6±0.42	0.30	0.33	0.38

Table 2: Results of inter-ELM power balance calculations for the JET-C and JET-ILW pulses, where $\mathfrak{F}_x = P_x/P_{Abs}$ is the fraction of power in each loss-channel x.

Approximately double the fraction of power is radiated in JET-ILW compared to that in the JET-C pulses, while the fraction \mathfrak{F}_{ELM} of time-averaged ELM power $\langle P_{ELM} \rangle$ is lower in the JET-ILW pulses, despite the higher ELM frequency (~ 3×) due to the lower ELM energy losses ΔW_{ELM} , i.e. ~ 0.05-0.25 MJ in JET-ILW c.f. ~ 0.3-0.6 MJ in JET-C pulses. In the JET-ILW pulses, P_{sep}^{IELM} ~ 12 MW is about twice that in the JET-C pulses (~ 6 MW). Although the fraction of power due to inter-ELM pedestal transport \mathfrak{F}_{Sep} ~ 0.3-0.4 is similar with both walls, the

absolute inter-ELM loss power P_{sep}^{iELM} in the JET-ILW pulses due to heat transport across the ETB is about twice that in the JET-C pulses despite the similar pedestal pressure.

In 3 MA JET-ILW pulses with more than 25 MW input power, bolometer tomography usually reveals a highly asymmetric total emissivity, e.g. as shown in Fig. 4 (a), predominantly from the mantle region, ($\rho_N > 0.7$). As derived by Wesson in Ref. 6, the redistribution of impurity ions x within a flux surface due to toroidal rotation Ω_{ϕ} is described by an expression of form:

$$n_x/n_{x0} = exp\{\mathcal{O}(1) m_x \Omega_{\phi}^2 / 2T_x (R^2 - R_0^2)\}$$

i.e. heavy impurities are flung to larger radius by the centrifugal force. Using expressions appropriate for a trace, heavy impurity [6] (Ni: $m_x/m_p \sim 59$ or W:184), a main impurity (Be), Ω_{ϕ} as measured by CXRS at the flux surface and assuming the heavy impurity dominates the radiation, the relative emissivity profile $\varepsilon(\theta)$ / $\varepsilon(\theta=0)$ is calculated, as shown in Fig. 4 (b). Clearly, in this high-power pulse, the distribution is consistent with a dominant W impurity.

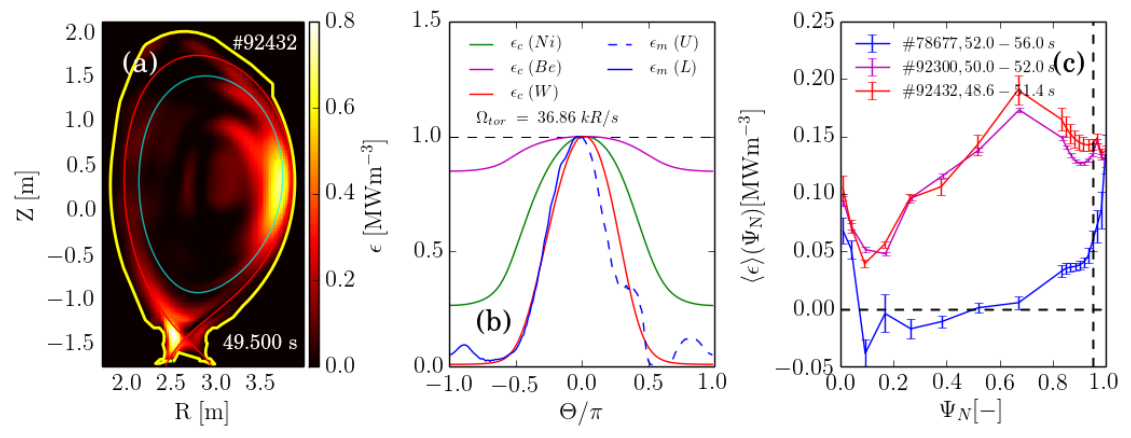


Fig. 4 (a) Total emissivity $\varepsilon(R,Z)$ for JET-ILW 3.0 MA pulse #92432 from bolometer tomography at 49.5 s, showing the separatrix 'red' and $\psi_N = 0.8$ 'cyan'); (b) normalised measured emissivity $\varepsilon_m(\theta)$ around the $\psi_N = 0.8$ contour shown in (a) ($\theta > 0$ above mid-plane) and calculated profiles $\varepsilon_c(\theta)$ for Be (magenta), W (red) and Ni (green) impurities and (c) flux-surface averaged emissivity profiles $\langle \varepsilon_m \rangle (\psi_N)$ for three of the pulses in Table 1, including a JET-C pulse for comparison, which doesn't exhibit the strong mantle radiation.

Using atomic data from ADAS [7] and the measured T_e profile, the dominant charge state in the mantle would be W²⁵⁻³⁰⁺, with estimated peak (mean) concentrations of 6 (1.5) ×10⁻⁴, contributing $\Delta Z_{eff} \sim 0.5$ (0.14) and fractional mass $\Delta \rho_m \sim 4$ (1) %. Mid-plane, VUV spectroscopy reveals strong emission over spectral regions at ~19±2 and 29±2 nm, associated with radiation from W²⁴⁻²⁶⁺, with peak abundance at ~1-2 keV typical of the mantle region [8].

Analysis of TS profile data reveals that the parameter $\eta_{NC} = R/L_n - R/2L_T$, which is proportional to the neo-classical, radial pinch velocity [9] is typically weakly outwards (~ 2) in the mantle and strongly inwards (~ -200) in the ETB, usually localising the sputtered W to the mantle region. However, in some pulses, η_{NC} reverses sign in the mantle causing the W to accumulate in the plasma core, terminating the ELMy H-mode phase of the pulse.

Analysis of bolometer data for the 1.4 MA JET-ILW pulses discussed above does not reveal the presence of similar strong, W radiation from the mantle region in these lower power pulses, in which the radiated power fraction decreases ($\mathfrak{F}_{Rad} \sim 0.4 \rightarrow 0.25$) with increasing power and the mid-plane radial emissivity $\varepsilon(R)$ distribution has a form like that in JET-C (fig. 4 (c)).

This work has been carried out within the framework of the EUROfusion Consortium and has received funding from the Euratom research and training programme 2014-2018 under grant agreement No. 633053 and from the RCUK Energy Programme [grant number EP/I501045]. The views and opinions expressed herein do not necessarily reflect those of the European Commission.

[1] Hatch D.R. et al., Nucl. Fus. **57** (2017) 036020; [2] Kotchenreuther M. et al., Nucl. Fus. **57** (2017) 064001; [3] Challis C. D. et al., Nucl. Fus. **55** (2015) 053031; [4] Maggi C. F. et al., Nucl. Fus. **55** (2015) 113031; [5] Maggi C. F. et al., Nucl. Fus. **57** (2017) 11612; [6] Wesson J.A., Nucl. Fus., **37** (1997) 578; [7] Henderson S. et al. PPCF **59** (2017) 055010; [8] T. Pütterlich, PPCF **50** (2008) 085016; [9] Angioni C. and Helander P., PPCF **56** (2014) 124001.